European Journal of Neuroscience, Vol. 12, pp. 4093–4106, 2000

A model of gamma-frequency network oscillations induced in the rat CA3 region by carbachol *in vitro*

Roger D. Traub,[1] Andrea Bibbig,[2*] André Fisahn,[3*] Fiona E. N. LeBeau,[4] Miles A. Whittington[4] and Eberhard H. Buhl[3,4]

[1]Division of Neuroscience, University of Birmingham School of Medicine, Edgbaston, Birmingham B15 2TT, UK
[2]Abteilung Neuroinformatik, Universität Ulm, D-89069, Ulm, Germany
[3]MRC Anatomical Neuropharmacology Unit, Oxford University, Oxford OX1 3TH, UK
[4]School of Biomedical Sciences, The Worsley Building, University of Leeds, Leeds LS2 9NL, UK

Keywords: 40 Hz, antidromic spike, carbachol, gamma oscillation, gap junction, hippocampus

Abstract

Carbachol (> 20 μM) and kainate (100 nM) induce, in the *in vitro* CA3 region, synchronized neuronal population oscillations at ≈ 40 Hz having distinctive features: (i) the oscillations persist for hours; (ii) interneurons in kainate fire at 5–20 Hz and their firing is tightly locked to field potential maxima (recorded in s. radiatum); (iii) in contrast, pyramidal cells, in both carbachol and kainate, fire at frequencies as low as 2 Hz, and their firing is less tightly locked to field potentials; (iv) the oscillations require $GABA_A$ receptors, AMPA receptors and gap junctions. Using a network of 3072 pyramidal cells and 384 interneurons (each multicompartmental and containing a segment of unmyelinated axon), we employed computer simulations to examine conditions under which network oscillations might occur with the experimentally determined properties. We found that such network oscillations could be generated, robustly, when gap junctions were located between pyramidal cell axons, as suggested to occur based on studies of spontaneous high-frequency (> 100 Hz) network oscillations in the *in vitro* hippocampus. In the model, pyramidal cell somatic firing was not essential for the oscillations. Critical components of the model are (i) the plexus of pyramidal cell axons, randomly and sparsely interconnected by gap junctions; (ii) glutamate synapses onto interneurons; (iii) synaptic inhibition between interneurons and onto pyramidal cell axons and somata; (iv) a sufficiently high rate of spontaneous action potentials generated in pyramidal cell axons. This model explains the dependence of network oscillations on $GABA_A$ and AMPA receptors, as well as on gap junctions. Besides the existence of axon–axon gap junctions, the model predicts that many of the pyramidal cell action potentials, during sustained gamma oscillations, are initiated in axons.

Introduction

Synchronized gamma-frequency (30–100 Hz) oscillations, in networks of cerebral neurons, may be important for perception (Roelfsema *et al*., 1994) and memory (Whittington *et al*., 1997b). Gamma oscillations occur *in vivo* in a number of situations and contexts (reviewed in Traub *et al*., 1999a). Two broad types of gamma oscillations *in vivo* include 'transient', lasting hundreds of ms to 1 or 2 s; and 'persistent', lasting many seconds or even minutes. Examples of transient oscillations include (i) those evoked by a brief sensory stimulus, such as a moving bar in the visual field (Gray & Singer, 1989), and (ii) those occurring (apparently) spontaneously in somatosensory cortex (MacDonald *et al*., 1996). An example of persistent gamma *in vivo* would be the spontaneous fast oscillations which occur superimposed on theta-frequency EEG waves in the hippocampus (Soltesz & Deschênes, 1993). In this latter form of gamma, identified hippocampal basket cells fire at gamma frequencies (Sik *et al*., 1995), while, in contrast, most pyramidal cells fire at low rates (Csicsvari *et al*., 1998). As certain types of hippocampal theta rhythm are dependent on muscarinic receptors (Kramis *et al*., 1975), it seems possible that persistent hippocampal gamma rhythms *in vivo* might depend on a cholinergic input from the septum, at least under some conditions. Experimental models of gamma oscillations have been developed in hippocampal slices. Again, they can be divided into 'transient' (hundreds of ms to a few seconds) and 'persistent' varieties. Transient oscillations can be evoked by activation of metabotropic glutamate receptors (GluRs), via application of glutamate or of trans-ACPD [(1S,3R)-1-aminocyclopentane-1,3-dicarboxylic acid], or by nearby brief electrical stimulation (Whittington *et al*., 1995; Traub *et al*., 1996b; Whittington *et al*., 1997a). In these cases, metabotropic GluRs excite neuronal populations to fire repetitively by depolarizing cell membranes and by blockade of spike frequency adaptation, through reduction of membrane K^+ conductances; synaptic conductances shape the form of the oscillation. The oscillation is transient because the neuronal excitation lasts only a finite time, presumably because of glutamate uptake and/or metabotropic GluR desensitization. Transient oscillations can also be evoked in pharmacologically isolated networks of interneurons (Whittington *et al*., 1995), and oscillations lasting seconds or longer can be evoked by puffs of hypertonic KCl solution (Towers *et al*. 2000).

Persistent gamma oscillations, evoked *in vitro* by bath application of carbachol (Buhl *et al*., 1998; Fisahn *et al*., 1998) or kainate, have

Correspondence: Dr Traub, as above.
E-mail: r.d.traub@bham.ac.uk

**Present address*: Andrea Bibbig, as for RDT; André Fisahn, Laboratory of Cellular and Molecular Neuroscience, NIH, Building 49 Rm. 5A72, Bethesda, MD, 20892 USA

Received 7 April 2000, revised 9 August 2000, accepted 21 August 2000

TABLE 1. Gamma oscillation phenomena: carbachol compared with tetanic stimulation

	Carbachol	Tetanic stimulation
Preferred Region	CA3	CA1
Duration	Minutes to hours	Hundreds of ms
Slow depolarization	Absent	> 10 mV in pyramidal cells and interneurons
Firing pattern of pyramidal cells	Statistically locked to field Frequency << population	Population spikes Frequency = population
Firing pattern of interneurons (kainate, 100 nM)	Locked to field Frequency ≈ ½ population	Locked to field Frequency = 1–2 × population
mGluR	Not required	Required
NMDA-R	Not required	Some contribution
AMPA-R	Essential	Some contribution
$GABA_A$-R	Essential	Essential
Gap junctions	Essential	Not required*

References: Fisahn *et al*., 1998; Whittington *et al*., 1997a; and Traub *et al*. (1999d). *M. A. Whittington, unpublished data.

different properties than the transient gamma oscillations evoked by tetanic electrical stimulation (Table 1). [Note, however, that in some laboratories, carbachol gamma oscillations have also been found to be transient (Fellous & Sejnowski, 2000).] For example, in the presence of carbachol or kainate, pyramidal cells are somewhat depolarized (< 5 mV, vs. 23 ± 2 mV after tetanic stimulation), but most interneurons are not significantly depolarized (0–1 mV, vs. 17 ± 2 mV after tetanic stimulation; E.H. Buhl, unpublished data; Whittington *et al*., 1997a). In addition, neither pyramidal cells nor interneurons fire as fast as the net population frequency with, however, interneurons (5–30 Hz) approaching the population frequency much more than the pyramidal cells (frequency often ≈ 2 Hz). Persistent gamma oscillations have one further important feature: they are suppressed by compounds that block gap junctions (Traub *et al*., 1999d; see also Results). It is the purpose of this study to define, in network simulations, conditions under which gamma oscillations can persist in a manner that depends on AMPA (α-amino-3-hydroxy-5-methyl-4-isoxazole propionic acid) and $GABA_A$ receptors, along with gap junctions. Gamma oscillations, in networks of pyramidal cells and interneurons and depending on chemical synaptic interactions without gap junctions, have been studied previously in simulations (Traub *et al*., 1997; Whittington *et al*., 1997a; Traub *et al*., 1999b). We need, however, to review briefly recent studies on gap junctions in the hippocampus and their apparent effects on network behaviour.

Gap junctions were included in the present network model because pharmacological blockade of gap junction conductance suppresses the gamma oscillations induced by carbachol. A question arising was: where to locate the gap junctions? In this matter, we were guided by studies of transient, spontaneous high-frequency (> 100 Hz) oscillations in hippocampal slices. Draguhn *et al*. (1998) showed that such oscillations were resistant to blockade of synaptic transmission by low-Ca^{2+} media, but were suppressed by three different gap junction blockers, and were augmented by ammonium chloride. Intracellular recordings from pyramidal cells demonstrated 'spikelets' (fast potentials usually < 9 mV in amplitude) as well as full action potentials, in phase with extracellular sharp potentials. In computer simulations of pairs of pyramidal cells, it was possible to replicate spikelets when gap junctions were placed between axons, with conductance large enough for an axonal spike in one cell to induce, across the junction, a spike in the coupled axon. Further studies (Traub *et al*., 1999c) have shown that (i) in simulations, transient, synchronized high-frequency oscillations would emerge, remarkably, in a network of pyramidal cells that was sparsely interconnected by axon–axon gap junctions, in the absence of chemical synapses; (ii) based on physiological experiments, the axon–axon gap junctions between hippocampal pyramidal cells are probably located not far from the axon initial segment (D. Schmitz, S. Schuchmann, A. Fisahn, A. Draguhn, E.H. Buhl, R.E. Petrasch-Parwez, U. Heinemann, R.D. Traub, unpublished data).

The present model, then, represents a synthesis of two types of model: one in which synaptic interactions shape a gamma oscillation, and one in which gap junctions shape a faster oscillation. The model to be described generates a population output at gamma frequency, wherein the firing patterns of individual cells resemble those recorded experimentally. We have recently shown (Traub & Bibbig, 2000) how axon–axon gap junctions, in combination with chemical synapses, might account for high-frequency (≈ 140–200 Hz) ripples superimposed upon sharp waves in the *in vivo* hippocampus (Ylinen *et al*., 1995). Some of these data have appeared in abstract form (Traub *et al*., 1999d).

Materials and methods

Experimental methods

Young adult Wistar rats were anaesthetized with inhaled isoflurane immediately followed by an intramuscular injection of ketamine (100 mg/kg) and xylazine (10 mg/kg). When all responses to noxious stimuli, such as tail pinch, had completely subsided the animals were perfused intracardially with ≈ 50 mL of modified artificial cerebrospinal fluid (ACSF) which was composed of (in mM) 252 sucrose, 3.0 KCl, 1.25 NaH_2PO_4, 24 $NaHCO_3$, 2.0 $MgSO_4$, 2.0 $CaCl_2$ and 10 glucose. Following brain removal, 450-μm-thick slices were cut in either the horizontal or coronal plane. Those sections containing hippocampus were transferred to either a holding or a recording chamber where they were maintained at either room temperature or, for recording purposes, at 34 °C at the interface between oxygenated ACSF and a mixture of 95% O_2 and 5% CO_2. After 30–45 min in modified ACSF all sucrose was replaced with equiosmolar (126 mM) NaCl and recordings commenced following an additional recovery period of ≈ 45 min. Extracellular recording electrodes were pulled from borosilicate glass tubing and filled with ACSF, with pipette resistances generally ranging from 2 to 5 MΩ. Those micropipettes manufactured for intracellular recordings were filled with 1.5 M KCH_3SO_4 and had resistances varying from 70 to 130 MΩ. Both extra- and intracellular recordings were made with an Axoprobe amplifier (Axon Instruments, Foster City, CA, USA) and permanently acquired with a DTR-1402 digital audio tape recorder (Biologic, Claix, France). Data analysis was continued off-line by (re)digitizing the data at 10 kHz, low-pass filtering the traces between 0.2 and 5 kHz with an eight-pole Bessel filter employing Axograph (Axon

Instruments) software. For further technical details see Fisahn *et al*. (1998). Drugs were purchased from Sigma (UK) and were diluted directly from stock solutions into the superfusion medium.

Overall structure of the network model

The computer program used in the present simulations was adapted from one used to study gamma and beta frequency oscillations induced by tetanic stimulation (Traub *et al*., 1999b). The network model consists of two overlapping rectangular arrays: 96×32 pyramidal cells (3072 total pyramidal cells) and 96×4 interneurons (384 total interneurons), intended to represent 1.92 mm of *in vitro* hippocampal tissue along s. pyramidale. Each neuron (pyramidal and inhibitory) is simulated with a multicompartment axon/soma/dendritic model. The network program simulates chemical synaptic interactions mediated by $GABA_A$ and AMPA receptors [NMDA receptors are known not to be essential for carbachol-induced oscillations (Fisahn *et al*., 1998)]. In addition, the model simulates interactions mediated by gap junctions, hypothesized to be located between axons of pyramidal cells (Draguhn *et al*., 1998; D. Schmitz, S. Schuchmann, A. Fisahn, A. Draguhn, E. H. Buhl, R. E. Petrasch-Parwez, R. Dermietzel, U. Heinemann and R. D. Traub, unpublished data). The model contains no gap junctions between soma-dendritic membranes of pyramidal cells, nor between interneurons. We are aware, however, that one group has reported a decrease, in spikelet frequency and of dye coupling between pyramidal cells, that is induced by carbachol (Perez Velazquez *et al*., 1997).

Metabotropic cholinergic effects were simulated by various factors. (i) Postsynaptic actions consisting of a tonic depolarizing conductance on pyramidal cells (Benson *et al*., 1988), and a rather small tonic conductance, as described to occur on parvalbumin-positive interneurons in the presence of cholinergic agonists (Kawaguchi, 1997). Cholinergic depolarization, perhaps via nicotinic receptors, has been described for nonparvalbumin-positive interneurons (Kawaguchi, 1997; Frazier *et al*., 1998), and for CA1 lacunosum/moleculare interneurons by muscarinic receptors (Chapman & Lacaille, 1999), but this effect is not included in the model. The reason is that gamma oscillations in our model are primarily gated by the parvalbumin-positive basket cells and axo-axonic cells, rather than by dendrite-contacting interneurons. (ii) Reduction in strength of unitary pyramidal/pyramidal EPSPs (Segal, 1989; Scanziani *et al*., 1995). (iii) Suppression of g_{Ca}, the slow Ca^{2+}-mediated afterhyperpolarization (AHP) conductance (Gähwiler & Brown, 1987; Cole & Nicoll, 1984), and the leak conductance (Madison *et al*., 1987). (iv) Suppression of 'A' conductance [the transient, inactivating K conductance (Nakajima *et al*., 1986)]. We did, however, include a noninactivating transient K conductance, 'D' conductance (Storm, 1988), because of evidence that 50 μM 4AP suppresses carbachol-induced gamma oscillatons, prior to the occurrence of epileptiform bursts (E.H. Buhl, unpublished data). (v) We also postulated the occurrence of spontaneous depolarizing events in axons, which lead to synaptic potentials and sometimes to axonal action potentials (ectopic spikes; see below), that can propagate antidromically or across gap junctions to other axons (whence they can further propagate orthogradely, antidromically or across more gap junctions). Carbachol could, in principle, augment the excitability of axons, given that it slows the inactivation of Na^+ channels (Cantrell *et al*., 1996), and that muscarinic receptors are present on axons (Levey *et al*., 1995).

We presume that the metabotropic actions of kainate are similar to those of carbachol (e.g. Rodriguez-Moreno & Lerma, 1998), but data concerning postsynaptic kainate effects on intrinsic conductances appear to be limited (Gho *et al*., 1986). The data base consisted of >118 preliminary simulations, followed by 24 further simulations performed once a basic parameter set had been chosen (as used in Fig. 1).

Structure and intrinsic properties of individual model neurons

The CA3 pyramidal cell model is based on that of Traub *et al*. (1994), with certain modifications as described below. This model has a soma, 63 compartments for the branching apical and basilar dendrites, an axon initial segment (75 μm long, radius 2 μm), and four cylindrical compartments of unmyelinated axon (each with length 75 μm, radius 0.5 μm). In its initial form, active conductances for soma/dendritic membrane were an inactivating g_{Na}, $g_{K(DR)}$ (delayed rectifier), a high-voltage-activated noninactivating g_{Ca}, a voltage- and Ca^{2+}-dependent fast K conductance $g_{K(C)}$, a slow Ca^{2+}-dependent afterhyperpolarization conductance, $g_{K(AHP)}$, and a transient, inactivating K conductance, $g_{K(A)}$. These conductances were distributed nonuniformly over the membrane. The initial segment and axon contained only g_{Na} and $g_{K(DR)}$; there was, in particular, no $g_{K(A)}$ in the axon (see, however, Debanne *et al*., 1997). R_m was 50 kΩ/cm^2 over the soma/dendritic membrane. In this model, somatic or dendritic depolarizing currents initiated Na^+ spikes in the axon initial segment, that propagated orthodromically and also retrogradely; the pattern of retrograde conduction ('backpropagation') was influenced by the spatial distribution of synaptic conductances.

In the present simulations, the following modifications were made to the intrinsic conductances of pyramidal cell soma/dendritic membrane, in part to account for carbachol actions:

(i) g_{Ca} and Ca^{2+}-dependent conductances were effectively eliminated by multiplying maximal g_{Ca} density by 10^{-4} (Gähwiler & Brown, 1987; Madison *et al*., 1987; but see Knöpfel *et al*., 1990).

(ii) Leak conductance was halved (i.e. R_m was multiplied by 2).

(iii) A persistent Na^+ conductance, $g_{Na(P)}$ (French *et al*., 1990), was added to the dendritic membrane, but not to the somatic membrane (Mittman *et al*., 1997). $g_{Na(P)}$ had activation kinetics as for g_{Na}, but no inactivation. The density of $g_{Na(P)}$ conductance in dendrites was equal to that of transient g_{Na} in the dendrites.

(iv) The density of transient K^+ conductance was made uniform at 0.25 mS/cm^2, and this conductance was altered so as to be noninactivating (Nakajima *et al*., 1986; Storm, 1988).

The intrinsic properties of model axons were not altered. Interneurons were simulated as in Traub & Miles (1995) except that in most, but not all, simulations, the excitability of dendrites was reduced by multiplying g_{Na} and $g_{K(DR)}$ densities in the dendrites by 0.1. These model interneurons show little firing-frequency adaptation in response to a steady injected current, and fire spontaneously (in the absence of external input) at ≈25 Hz; the spontaneous firing frequency, however, is quite sensitive to membrane potential (Traub & Miles, 1995). All of the interneurons in the model network have identical intrinsic properties. This, of course, represents a simplification of the actual biology (e.g. Maccaferri & McBain, 1996). The interneurons are distinguished, however, by their connectivity patterns and, in some cases, by the time courses of the inhibitory postsynaptic conductances (IPSCs) induced by single presynaptic action potentials.

Connectivity of chemical synaptic interactions

The 384 interneurons were divided into four types, with 96 interneurons of each type: 'axo-axonic cells' which contacted the initial segment of pyramidal cells, but which did not contact other interneurons; 'basket cells' which contacted the soma and most proximal dendrites of pyramidal cells; 'bistratified cells' which contacted the basilar dendrites and mid-apical dendrites of pyramidal

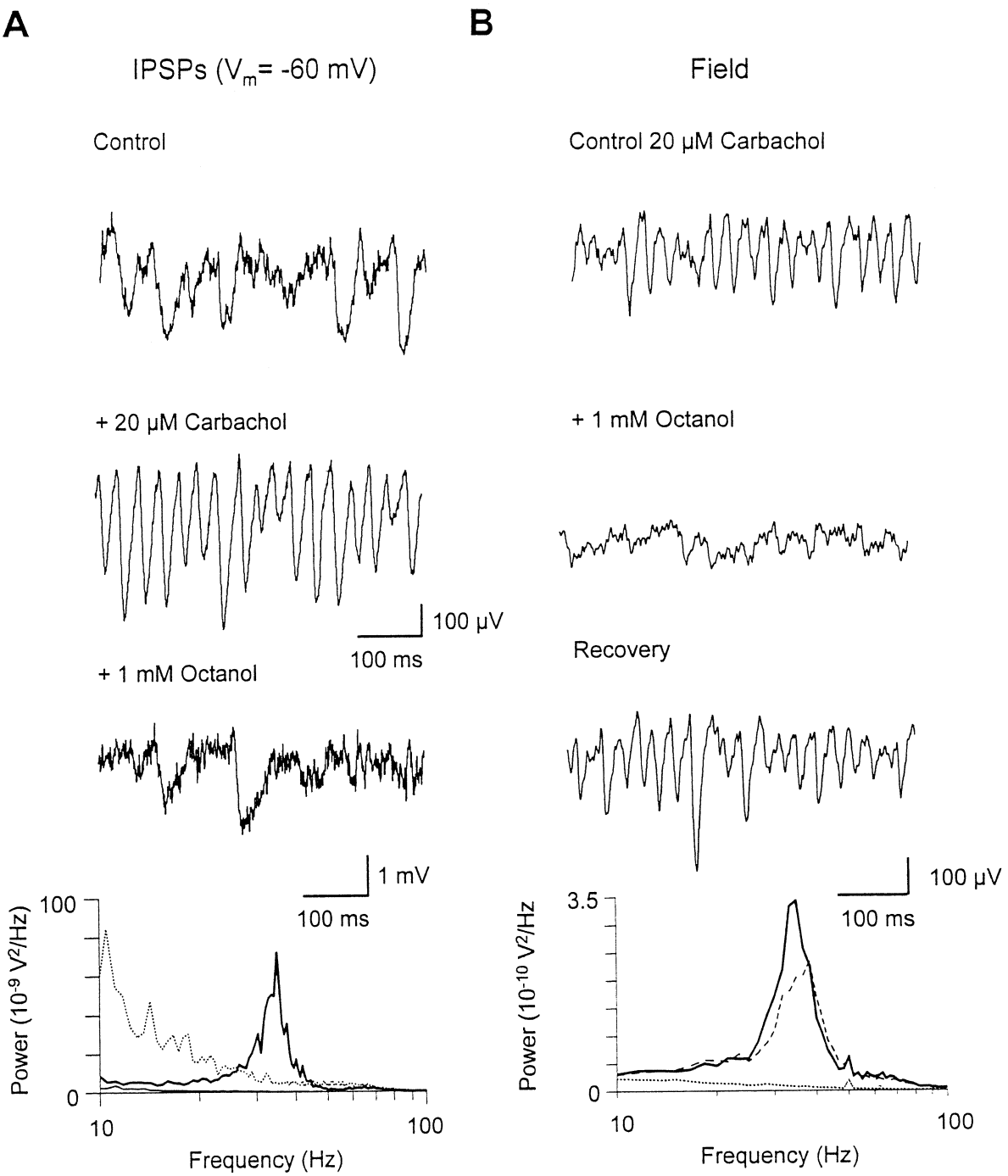

FIG. 1. Carbachol-evoked extra- and intracellular gamma frequency oscillatory activity was abolished by the gap junction uncoupling agent octanol. (A) Intracellular current clamp recording of a CA3 pyramidal cell in control solution (top trace), following 20 μM carbachol application (middle trace) and in the additional presence of 1 mM octanol (bottom trace). (B) Extracellular field recordings from the hippocampal CA3 area. The field pipette was positioned near the border region of strata radiatum and lacunosum-moleculare. In the presence of carbachol (20 μM), gamma frequency oscillations were present that were completely abolished 20 min after bath application of octanol (1 mM). Following wash of octanol, the gamma frequency activity fully recovered. The power spectra below show the responses with carbachol (solid line), during octanol application (stippled line) and following wash of octanol (dashed line). A clear peak in the spectrum, in the gamma frequency range, is evident during both control and recovery.

cells; and 'o/lm' cells which contacted the distal apical dendrites of pyramidal cells. Inhibitory synapses for interneuron–interneuron connections were located in the dendrites. A presynaptic pyramidal cell contacted postsynaptic pyramidal cells and interneurons in a pattern that was random and independent of the location of the respective cells. A presynaptic interneuron contacted postsynaptic cells (pyramidal cells and interneurons) in a pattern that was also random but subject to a spatial constraint: the somata of pre- and postsynaptic cell had to be within 500 μm of each other along the long axis of the array. Pyramidal–pyramidal connections were made onto basilar dendrites, as would be likely to occur in that portion of CA3 bordering on CA1 (Li *et al.*, 1994). Each pyramidal cell had 30 presynaptic pyramidal cells and 80 presynaptic interneurons, 20 of each interneuron type. Each interneuron had 150 presynaptic

pyramidal cells and 60 presynaptic interneurons (20 of each type, exclusive of axo-axonic cells).

Kinetics of unitary synaptic conductances

Unitary excitatory synaptic conductances were simulated by alpha functions of the form $c_e t e^{-t/\tau}$, where $\tau = 2$ ms for synapses on pyramidal cells and 1 ms for synapses on interneurons; t was time from onset of the conductance and c_e a parameter. Unless specified otherwise, $c_e = 0.15$ nS on pyramidal cells, with values up to 0.6 nS used on occasion, and $c_e = 0.5$ nS on interneurons in most simulations. [Increases in interneuron c_e produced small changes in network frequency, once this parameter was above a threshold value.] Inhibitory synaptic conductances ($GABA_A$ receptor-mediated only) consisted of a step rise, followed by an exponential decay: $c_i e^{-t/\tau}$. τ was 6 ms for presynaptic axo-axonic and basket cells; the default value of τ for dendrite-contacting interneurons was also 6 ms (Pawelzik *et al*., 1998), but was 50 ms in some simulations (without significant impact on results, provided dendritic conductances were not too large). Other default values were: $c_i = 2$ nS for basket cell or axo-axonic cell → pyramidal cell connections; $c_i = 0.25$ nS for bistratified cell or o/lm cell → pyramidal cell connections; $c_i = 2$ nS for basket cell → interneuron connections; $c_i = 0.1$ nS for bistratified cell or o/lm cell → interneuron connections. For EPSPs, reversal potential was 60 mV positive to resting potential; for inhibitory postsynaptic potentials (IPSPs), it was 15 mV negative to resting. No provision was made for either short-term or long-term synaptic plasticity. Excitatory or inhibitory synaptic conductances, on a given compartment of a given postsynaptic cell, induced by firing of different presynaptic axons, were simply added together. The condition for eliciting a postsynaptic conductance was that the membrane potential of the most distal compartment of the presynaptic axon be depolarized 70 mV from rest. Synaptic transmission was 'faithful', i.e. not quantal.

Properties of gap junctions

Gap junctions were located between homotopic compartments of pyramidal cell axons: either the compartment just distal to the initial segment (most cases) or three compartments distal to the initial segment. For axons to have a possibility of being connected, the respective somata needed to be within 200 µm of each other. In addition, no axon was allowed to contact more than four other axons. Gap junctions were placed randomly between candidate pairs of axons. The default probability of inserting a gap junction was such that each axon contacted, on average, 1.6 other axons. This probability was chosen because it falls in a range of gap junction densities found, in simulations, to be capable of replicating high-frequency population oscillations (Draguhn *et al*., 1998; Traub *et al*., 1999c). As described in Traub *et al*. (1999c), and following the classical work of Erdös & Rényi (1960), such a low density of gap junctions does not lead to a syncytium in which any pyramidal cell is connected 'poly gap-junctionally' to any other pyramidal cell. (Note, in contrast, that the chemical excitatory synaptic network in the model is fully connected: any pyramidal cell is connected, polysynaptically, to any other pyramidal cell.) Instead, in the gap junction network, there is a 'large cluster' consisting of ≈2/3 of the pyramidal cells, which is 'poly gap-junctionally' connected. The remaining ≈1/3 of the pyramidal cells are either gap-junctionally isolated (i.e. the axon contacts no other axon) or else are part of small clusters, mostly of size 2 or 3 cells. Simulated gap junctions did not rectify and the conductance was independent of voltage. The default value of the junctional conductance was 191 MΩ, large enough for a spike in one axon to induce a spike (after an ≈0.25-ms delay) in a coupled axon. Such spike transduction was not guaranteed, however, and might be prevented by shunting (synaptic or by intrinsic conductances) of the membrane. As shown previously (Traub *et al*., 1999c), axonal spikes propagating antidromically could induce at the soma either a full spike (generally inflected on the rising phase), a 'partial spike' of ≈10–20 mV (occurring when the antidromic spike invaded as far as the initial segment), or a 'spikelet' of ≈3 mV (occurring when the antidromically propagating axonal spike only reached the axonal membrane just distal to the initial segment).

Ectopic axonal spikes

Evidence has accrued that ectopic axonal spikes occur in at least two experimental *in vitro* epilepsy models, an acute 'kindling' model produced by electrical stimulation (Stasheff *et al*., 1993), and in the 4AP model (Traub *et al*., 1995; Avoli *et al*., 1998). Simulations suggest that ectopic spikes could play a fundamental role in driving not only 4AP-induced population bursts, but also in driving (i) the so-called tertiary bursts during *in vitro* seizures in disinhibited slices (Traub *et al*., 1996a), (ii) high-frequency bursts *in vitro* (Traub *et al*., 1999c), and (iii) high-frequency ripples *in vivo* (Traub & Bibbig, 2000). Furthermore, in preliminary simulations of carbachol-induced gamma oscillations, when the main source of excitation in the network was in the form of tonic excitation of the neurons, sufficient to cause gamma-frequency oscillations, then the individual pyramidal cells would not fire at low rates, unlike experimental observations. For these reasons, ectopic spikes were included in the present model, and indeed had to occur at high rates for there to be population oscillations. Ectopic spikes were induced by current pulses (0.2 nA for pyramidal cells, 0.3125 ms) to distal axonal compartments of pyramidal cell and interneuron axons. The timing of the current pulses was random, with Poisson statistics, and statistically independent between neurons. The mean interval between pulses was fixed at 5 s for interneuron axons. For pyramidal cell axons, mean intervals of 15 ms to 2 s were used; in most simulations, the mean interval between ectopic pulses was 65 ms for each pyramidal cell axon.

Tonic synaptic conductances

Neurons were tonically excited with dendritic synaptic conductances (reversal potential 60 mV positive to rest) (Benson *et al*., 1988; Charpak *et al*., 1990). For pyramidal cells, the mean total conductance was usually 5 nS, with a 1-nS spread between different pyramidal cells (uniform probability distribution). Increasing the value of this conductance forced the pyramidal cells to fire on a larger proportion of the gamma waves; therefore, experimental observations on the sparseness of pyramidal cell firing force an experimental constraint on the parameter. For interneurons, the total tonic excitatory conductance was 0.0–0.2 nS. Again, there is an experimental constraint on the tonic excitation of the interneurons: if tonic excitation of interneurons is too large, then blocking AMPA receptor-mediated conductances will allow the interneuron network to generate autonomous oscillations (Traub *et al*. 1996b), contrary to the experimental observation that carbachol gamma oscillations collapse when AMPA receptors are blocked (Fisahn *et al*. 1998). The heterogeneity (spread) of driving conductances to interneurons was kept small, in most simulations, following the theoretical notion that pharmacologically isolated interneuron networks are not expected to tolerate much dispersion of tonic excitation if stable gamma oscillations are to be produced (Wang & Buzsáki, 1996; White *et al*., 1998). On the other hand, increasing five-fold the dispersion in driving conductances to interneurons did not change qualitative features of the simulated oscillation. This is expected, as the present

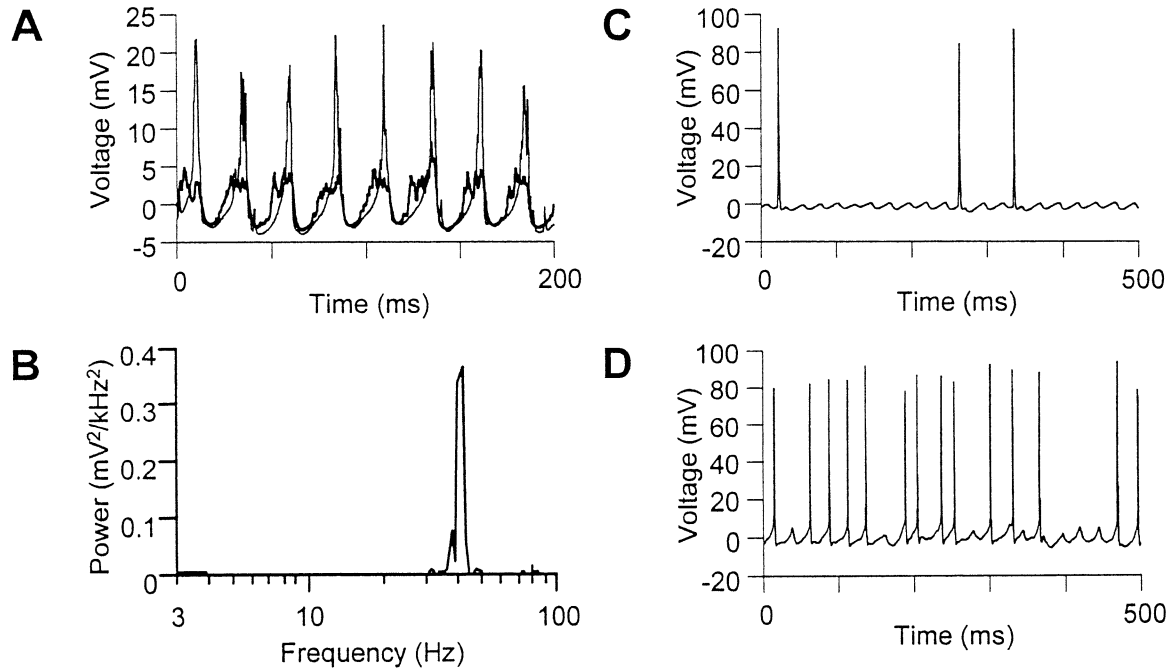

FIG. 2. Network model replicates basic experimental features of carbachol-induced gamma oscillations in CA3 region *in vitro*. (A) Average somatic membrane potentials of 28 nearby interneurons (thin line), and 224 nearby pyramidal cells (thick line), shows population oscillation. The average pyramidal cell peaks are broader than the average interneuron peaks, and pyramidal cell firing leads interneuron firing. (B) Power spectrum of the average pyramidal cell signal has a large peak at 42 Hz. (C) Pyramidal cell exhibiting subthreshold gamma frequency oscillation (produced by synaptic potentials, mainly IPSPs), with firing on a minority of the waves. (D) Interneuron fires on > 50% of the waves. Note the large EPSPs when the interneuron did not fire.

model depends on phasic AMPA receptor-mediated inputs to interneurons, and so is a structurally different model than an isolated interneuron network. We also did not include gap junctions between interneurons, presumably dendritic (Galarreta & Hestrin, 1999; Gibson *et al*., 1999; Fukuda & Kosaka, 2000; Tamás *et al*. 2000), even though preliminary simulations indicate that dendritic gap junctions between interneurons can stabilize gamma oscillations in isolated interneuron networks (R.D. Traub, A. Bibbig, M.A. Whittington and E.H. Buhl, unpublished data): the model to be presented worked without interneuronal gap junctions and, additionally, our preliminary simulations (with interneuronal gap junctions) were in networks of tonically depolarized interneurons, unlike the model used in this paper.

Axon conduction delays were calculated by the rule that pyramidal cell axons conduct at 0.5 m/s and interneuron axons at 0.2 m/s. The lattice spacing between neurons was 20 μm.

Technical aspects

The simulation program was written in FORTRAN, augmented by special instructions for a parallel computer, an IBM SP/2 with 12 processors, in the AIX operating system environment. Simulation of 1500 ms (the usual total time run) took ≈ 10.2 h. For detailed questions on the code, please send E-mail to: r.d.traub@bham.ac.uk. Power spectra were computed for 4096 data point epochs (768 ms), using a fast Fourier transform algorithm. In the figures, membrane voltages are plotted relative to resting potential.

Results

Octanol suppresses carbachol-induced gamma-frequency activity

Figure 1 illustrates intra- and extracellular recordings of 20 μM carbachol-induced gamma oscillatory activity, having an appearance similar to that described in Fisahn *et al*. (1998). The intracellular recording is from a pyramidal cell. This figure shows that the gap junction blocker octanol (1 mM) suppresses the oscillation. Similar

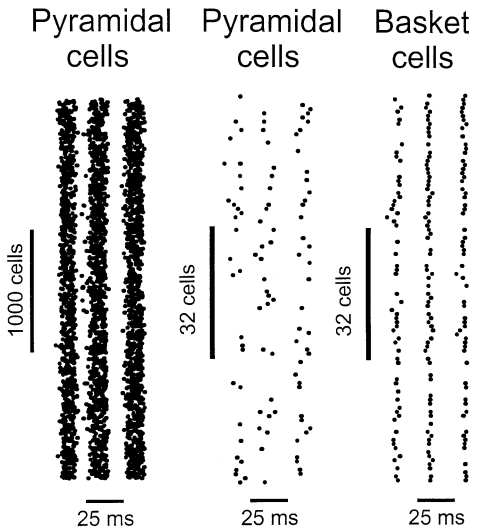

FIG. 3. Raster plots of simulated carbachol oscillation. Same simulation as Fig. 2. (Left) Three waves of the oscillation, with each dot representing a spike in one pyramidal cell. All 3072 pyramidal cells are plotted in this raster. The cells are ordered numerically (1,2, . . . 3072), but in the simulated array the cells are arranged in 32 rows of 96 cells each (i.e. Row 1, cells 1–96; Row 2, cells 97–192, etc.). This plot emphasizes the temporal spread of pyramidal cell firing, with an overall temporal organization. (Middle) Raster of 96 pyramidal cells, representing one row of the array. There was no obvious spatial structure to the activity, and cells skipped beats. (Right) Raster of the 96 basket cells. Again, there was no obvious spatial structure. Firing was 'denser' than for pyramidal cells, and temporally more precise.

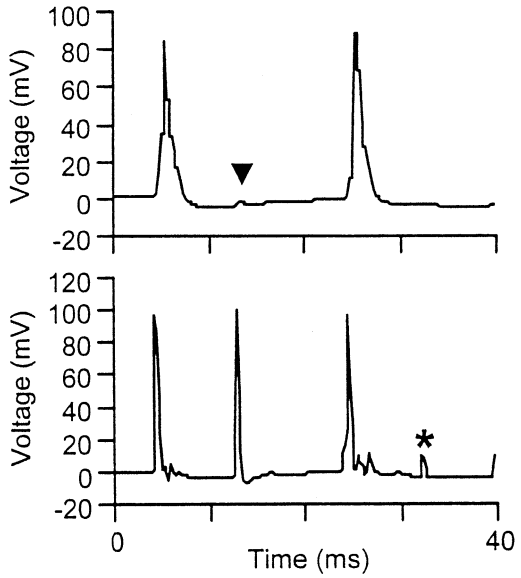

FIG. 4. Pyramidal cell action potentials in the model were antidromic. Same simulation as Fig. 2. Simultaneous trace of pyramidal cell soma (above) and axon just distal to initial segment of the same cell (below). Axonal spikes consistently lead somatic spikes. Note the somatic spikelet (arrow) occurring when an axonal spike blocks. The axon itself exhibited partial spikes (e.g. ★), resulting from action potentials in gap-junction-coupled axons that did not invade the illustrated axon.

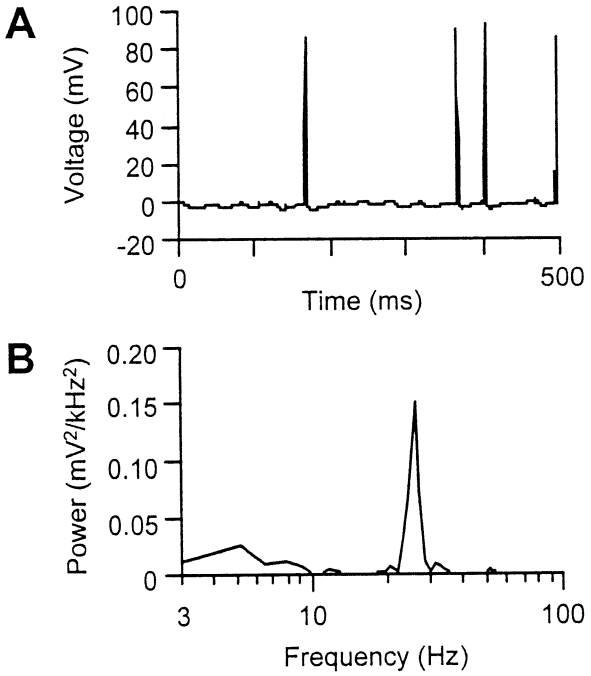

FIG. 5. Prolongation of $\tau_{GABA(A)}$ from 6 ms to 20 ms slowed the oscillation. Parameters otherwise as in Figs 2 and 3. (A) Single pyramidal cell. (B) Power spectrum of local average pyramidal cell voltage. Peak was at 26 Hz.

results were observed in five additional slices. The effect of octanol was reversible. We note that Draguhn *et al.* (1998) found that octanol did not affect the repetitive firing properties of a majority of pyramidal neurons tested.

In preliminary simulations, without ectopic axonal activity, it was found to be possible to produce network gamma oscillations by tonically exciting pyramidal cells and interneurons (cf. Traub *et al.*, 1997; Whittington *et al.*, 1997a), but not (so far as we could determine) with the pyramidal cells firing randomly and intermittently while at the same time having interneuron network gamma collapse with AMPA receptor blockade [as occurs experimentally (Fisahn *et al.*, 1998)]; nor could such preliminary simulations account for the effects of gap junction blockade.

We next showed that the model can generate population oscillations with properties as observed experimentally with carbachol in the CA3 region of the hippocampal slice, using 'default' values of the parameters, as defined in Materials and Methods. We then illustrated the effects of varying some of the important parameters. In some cases, the parameter variations correspond to experimental manipulations. In other cases, the parameter variations provide conceptual insight.

Gamma frequency population oscillations occur with firing frequencies of pyramidal cells being much lower than the population frequency. Figure 2 summarizes data from a simulation chosen using 'default' parameters. This simulation captures the following features of carbachol oscillations that have been described experimentally (Fisahn *et al.*, 1998; Traub *et al.*, 1999d): (i) the average behaviour of the system is oscillatory, with a sharp peak, at gamma frequency, in the power spectrum (Fig. 2A and B); (ii) in pyramidal cells, there is a clear subthreshold oscillation in membrane potential at gamma frequency. Action potentials generally occur on the peaks of the oscillatory waves, but only on a minority of the waves (Fig. 2C). Note, in addition, that (iii) interneurons fire at higher frequencies than pyramidal cells. Interneuron action potentials, when they occur, are

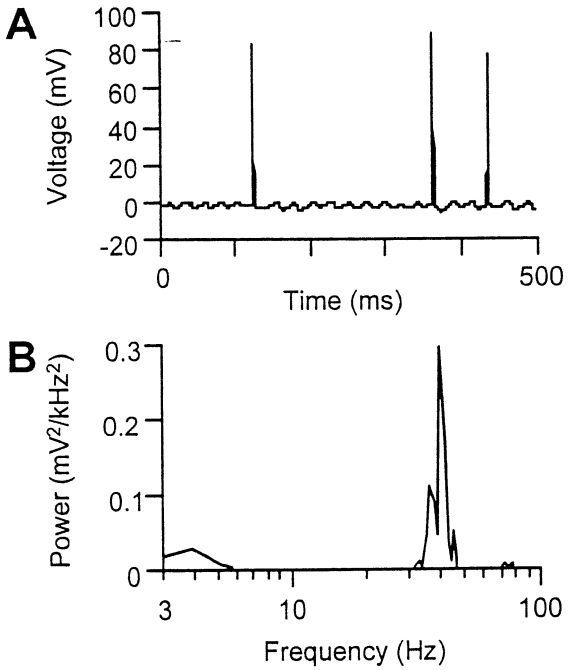

FIG. 6. Model: increasing all unitary $GABA_A$ conductances by 50% did not alter oscillation frequency in the population. Parameters otherwise as in Figs 2 and 3. (A) Single pyramidal cell. (B) Power spectrum of local average pyramidal cell voltage. Peak was at 40 Hz.

on the peaks of EPSPs (Fig. 2D); and (iv) the firing of interneurons is, on average, more tightly 'tuned' than is the firing of pyramidal cells, and the firing of pyramidal cells, on average, leads the firing of interneurons by a few ms (Fig. 2A). The gamma oscillations in this simulation were synchronized between opposite ends of the network

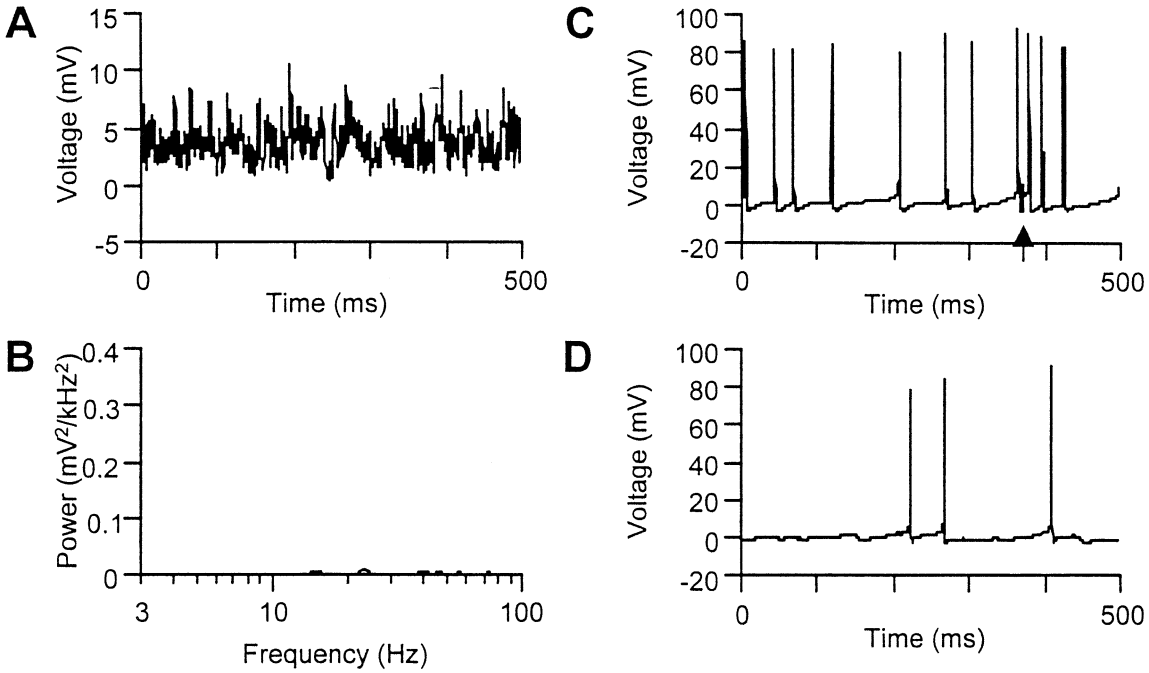

FIG. 7. Model: blocking AMPA receptors abolished the gamma oscillation. Parameters otherwise as in Figs 2 and 3. (A) Local average potential of 224 pyramidal cells. (B) Power spectrum of the signal in A. Note the absence of a gamma frequency peak (compare Fig. 2). (C) Individual pyramidal cell. Note absence of subthreshold gamma oscillation. Arrow indicates a partial spike. (D) Interneuron. Again, there was an absence of gamma-frequency EPSPs. The synaptic potentials did appear somewhat rhythmic, however, and the power spectrum of the average interneuron voltage (not shown) revealed a peak at 20 Hz.

(mean phase lag < 1 ms, data not shown). Simulated oscillations settled into a stable pattern after 1 or 2 cycles, and this pattern persisted for at least 1.5 s.

Figure 3 shows raster plots of activity taken from three cycles of the oscillation in the simulation of Fig. 2. The raster plots again show the apparent lack of spatial patterning (consistent with synchrony between activity at opposite ends of the array), the tighter temporal tuning of interneuron firing (as compared with pyramidal cells) and the relative sparseness of pyramidal cell firing.

Pyramidal cell action potentials are antidromic

A striking aspect of the simulation in Fig. 2 is that pyramidal cell axonal spikes (just distal to the initial segment), in all examples examined, occurred in advance of somatic spikes (Fig. 4). In the model, neither the tonic excitatory conductances nor recurrent EPSPs were sufficient, in themselves, to lead to action potentials. (Such action potentials, if they were to occur, would begin in the axon initial segment (Traub *et al*., 1994).) In contrast, ectopic axonal spikes (either originating in a cell's own axon, or else originating in another axon and propagating over one or more gap junctions), could invade somata from time to time. The invasion would depend on membrane potential and shunts in and near to the soma.

Prolonging $\tau_{GABA(A)}$ slows the oscillation

This effect has been observed experimentally in carbachol-induced gamma oscillations (Fisahn *et al*., 1998). The effect has also been observed in experiments (and simulations) in gamma oscillations in CA1 interneuron networks induced by metabotropic glutamate receptors (Whittington *et al*., 1995; Traub *et al*., 1996b) and in CA1 pyramidal cell/interneuron network oscillations induced by tetanic stimulation (Faulkner *et al*., 1998). Figure 5 shows that prolonging $\tau_{GABA(A)}$, from 6 ms (the value for Fig. 2) to 20 ms, slows the population frequency from 42 to 26 Hz. Other qualitative features of the oscillation did not appear to be affected.

Increasing $GABA_A$ conductances by 50% has little effect on the oscillation

A major effect of benzodiazepines is to increase $GABA_A$ conductance, although at large concentrations the time courses of GABA conductances are also affected. It has been found experimentally that benzodiazepines (specifically diazepam, clonazepam and midazolam) do not have significant effects on the frequency of gamma oscillations induced by carbachol or kainate (E. H. Buhl, unpublished data). In the model, likewise, when the simulation of Fig. 2 was repeated with all $GABA_A$ conductances increased by 50%, the oscillation persisted at 40 Hz, with intermittent pyramidal cell firing as before (Fig. 6). This result may be explicable in part as follows: $\tau_{GABA(A)}$ in the model was only 6 ms whilst the oscillation interval at 40 Hz would be 25 ms, or $> 4 \times \tau_{GABA(A)}$. The oscillation interval was therefore only partly determined by IPSC relaxation; build-up of excitatory activity also contributed (Fig. 2A), and this build-up itself takes time. In this situation, an increase in $GABA_A$ conductance would not be expected to influence the oscillation interval [to see this, note that $e^{-4} = 0.018 = 1.8\%$; a 50% increase in this quantity would only be 2.7%.] We note that diazepam, at concentrations up to $\approx 1.0\,\mu M$, has modest effects on the frequency of tetanically induced gamma oscillations (Faulkner *et al*., 1998); in pharmacologically isolated interneuron networks, however, 1.0 μM diazepam decreased oscillation frequency by almost 50% (Whittington *et al*., 1996). In the latter networks, of course, excitation of interneurons is presumed to be tonic, and there is no build-up of excitatory synaptic activity during each oscillation period, features distinguishing gamma in isolated interneuron networks from carbachol-induced gamma.

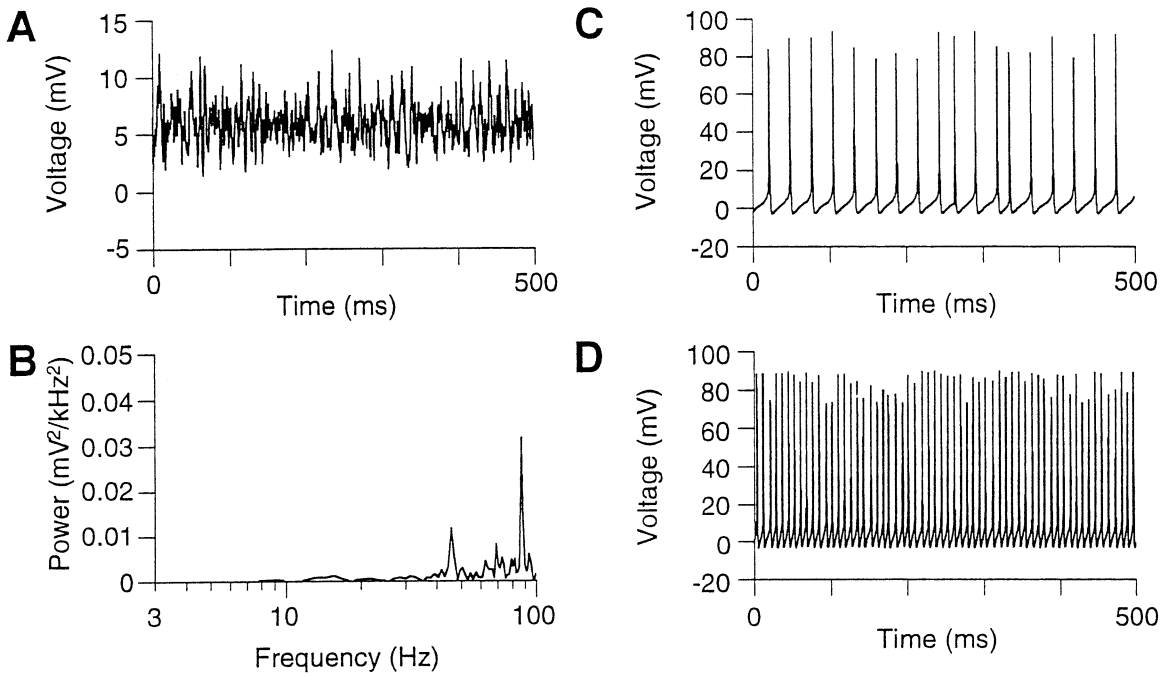

FIG. 8. Model: blocking $GABA_A$ receptors disrupted the gamma oscillation, and a higher frequency oscillation was unmasked. Parameters otherwise as in Figs 2 and 3. (A) Local average potential of 224 pyramidal cells. (B) Power spectrum of the signal in A. Peak is now at 87 Hz, and the amplitude of the peak is reduced more than 10-fold compared with Fig. 2. (C) Individual pyramidal cell. Note the rhythmic high-frequency firing. (D) Interneuron. Without the interneurons inhibiting each other, and with high-frequency AMPA-receptor input from the pyramidal cells, the interneurons fired rapidly (120 Hz in this case).

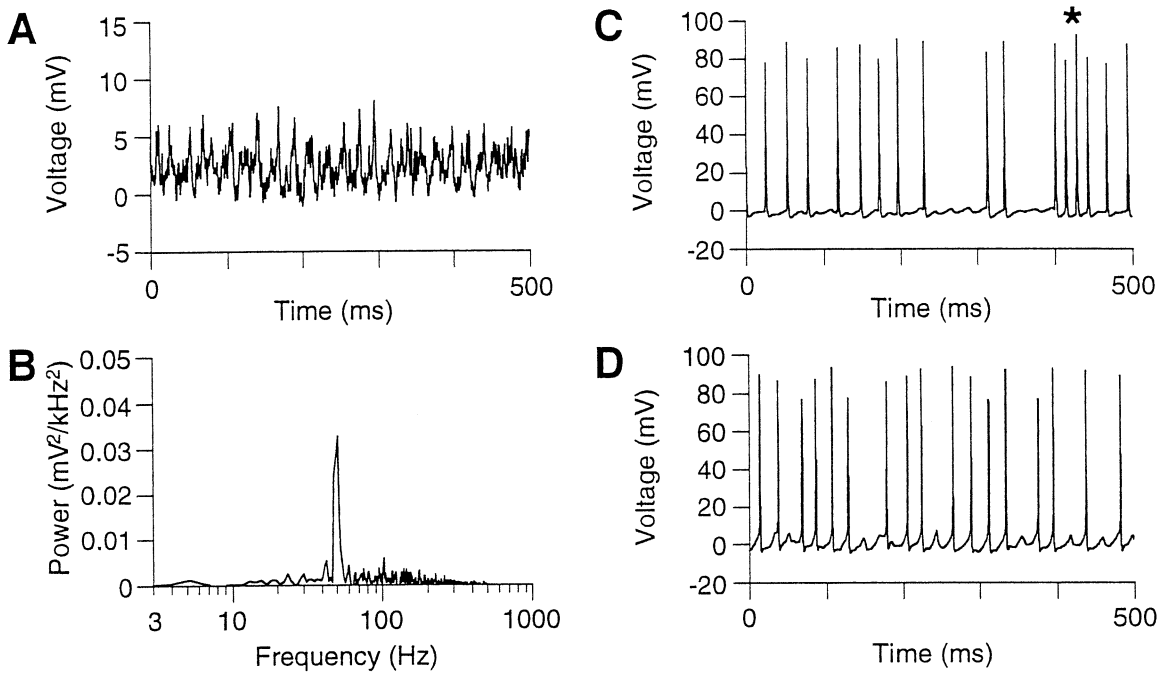

FIG. 9. Model: blocking $GABA_A$ receptors on pyramidal cell initial segments increased oscillation frequency, and increased the firing rate of individual pyramidal cells. Parameters otherwise as in Figs 2 and 3. (A) Local average potential of 224 pyramidal cells. The signal suggests the presence of multiple frequencies. (B) Power spectrum of the signal in A shows a peak at 51 Hz, but also power at higher frequencies. (C) Individual pyramidal cell. Action potentials occurred both on the peaks of gamma waves and also in high-frequency runs (e.g. ★). (D) Interneuron firing was qualitatively similar to that in Fig. 2.

Blocking AMPA receptors abolishes simulated carbachol-induced gamma oscillations

Fisahn *et al.* (1998) showed that carbachol-induced gamma oscillations were suppressed by pharmacological blockade of AMPA receptors; this finding was interpreted as implying a requirement either for (i) pyramidal cells to excite each other synaptically, and/or (ii) for glutamate release to occur onto interneurons and thereby excite them. In the simulation of Fig. 7, parameters were as in Fig. 2 with the exception that all AMPA conductances were set to zero. As in the experiment, the population oscillation was abolished. Blocking

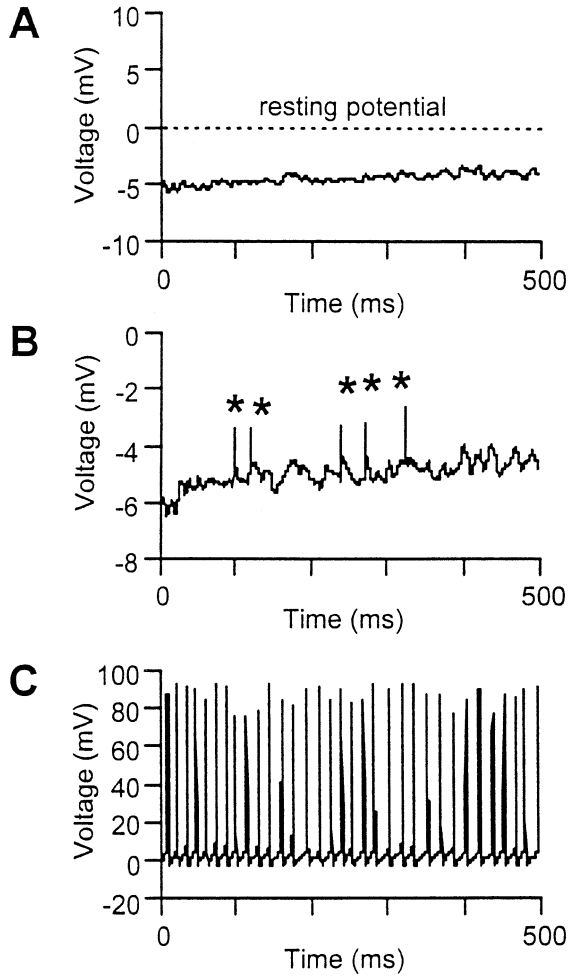

FIG. 10. Model: blocking $GABA_A$ receptors on interneurons lead to high-frequency firing of the interneurons and suppression of the pyramidal cell oscillation. Parameters otherwise as in Figs 2 and 3. (A) Local average potential of 224 pyramidal cells. Note the hyperpolarization and absence of oscillation. (B) Individual pyramidal cell. Blocked antidromic spikes are evident (★). (C) Interneuron. Note rapid firing (≈ 70 Hz).

AMPA receptors on pyramidal cells alone had little effect in our model, whilst blocking AMPA receptors solely on interneurons was sufficient to suppress the oscillation (not shown). Thus, in the model at least, it is synaptic excitation of interneurons, and not of pyramidal cells, which is a critical component of oscillatory activity.

Effects of blocking $GABA_A$ receptors

Fisahn *et al*. (1998) further showed that blockade of $GABA_A$ receptors would also abolish carbachol-induced gamma oscillations. The experimental application of bicuculline (1–10 μM), of course, would block $GABA_A$ receptors on both pyramidal cells and interneurons. In the simulation illustrated in Fig. 8, we repeated the 'experiment' of Fig. 2, but with all $GABA_A$ conductances set to zero (that is on both pyramidal cells and interneurons). In the power spectrum of local average pyramidal cell voltages (Fig. 8B), there is a small peak at 87 Hz, at < 10% of the amplitude of the 42 Hz peak (Fig. 2B); this residual rhythmicity probably results from the gap junction coupling between pyramidal cell axons in the model (Traub *et al*., 1999c; Traub & Bibbig, 2000). This fast oscillation might not be observable experimentally in bicuculline, as the drug appears to suppress ectopic axonal spikes (Stasheff *et al*., 1993), but a fast oscillation (≈ 100 Hz) is observable in carbachol when both $GABA_A$ and ionotropic glutamate receptors are blocked (Fisahn, 1999). The latter fast oscillation was blocked both by the gap-junction blocker octanol (1 mM) and by the PKC blocker chelerythrine (20 μM) (Fisahn, 1999). Note in Fig. 8 the high firing rates of both pyramidal cells and interneurons in this disinhibited model state, under conditions when pyramidal cell axons are spontaneously active.

Effects of blocking subsets of $GABA_A$ receptors

In order to provide further insight into the mechanism, we ran simulations in which $GABA_A$ receptors were blocked at specific sites, while all other parameters were as in Fig. 2. When $GABA_A$ receptors were blocked on pyramidal cell somata, proximal dendrites and axon initial segments, but not elsewhere (i.e. not on pyramidal cell distal dendrites, nor on interneurons themselves), then coherent population oscillations did not occur (not shown). When $GABA_A$ receptors were blocked only on pyramidal cell axon initial segments, however, gamma frequency oscillations occurred, although at higher frequency (51 Hz) and much lower power than in Fig. 2 (Fig. 9; note also the power at both higher and lower frequencies). Pyramidal cells fired on a higher percentage of the gamma waves under these conditions. For example, the pyramidal cell in Fig. 9C fired 41 times in 1.5 s, but the same cell fired only 14 times in 1.5 s in the simulation of Fig. 2. As pyramidal cell firing, in these simulations, is initiated in the axon distal to the initial segment, one can see that initial segment $GABA_A$ receptors are acting to regulate antidromic spike invasion, and thus the percentage of gamma waves which will be crowned with spikes. The pyramidal cell in Fig. 9C also exhibited a fast (≈ 65 Hz) run of antidromic action potentials (★); evidently, initial segment $GABA_A$ receptors could help to regulate this type of axon-network-generated activity as well.

Blocking $GABA_A$ receptors solely on interneurons

Blocking $GABA_A$ receptors solely on interneurons suppressed the gamma oscillation entirely, apart from a transient lasting < 200 ms (Fig. 10). Some degree of axonal firing persisted, as is evident from the spikelets in pyramidal cell somata (★ in Fig. 10B). Interneurons fired at ≈ 65 Hz, maintaining the pyramidal cell hyperpolarization.

Effects of blocking gap junctions

Pharmacological evidence indicates that carbachol-induced gamma oscillations depend upon gap junction conductances (Fisahn, 1999; Traub *et al*., 1999d; Fig. 1). We therefore examined the effects of blocking gap junction conductances in the model, maintaining all other parameters as in Fig. 2. This examination proceeded in stages, to search for transitional sorts of population behaviour that could be sought experimentally. For example, when gap junction conductances were uniformly reduced by 40%, a 40-Hz peak was clearly visible in the power spectrum of average activity (Fig. 11A and B), although at < 1/20 th the power of the simulation in Fig. 2. Examination of the average signal (Fig. 11A, ★) and of individual pyramidal cell traces (e.g. Fig. 11C, ★) indicates that short epochs of gamma oscillation occurred interspersed with periods of incoherent population activity. Further reduction of gap junction conductances (down 60% as compared to Fig. 2) abolished coherent population oscillations (Fig. 12).

The model generated gamma oscillations without axon–axon gap junctions, provided there was enough spontaneous ectopic activity in the axons. We were interested in the question of whether gap junctions were required, in principle, to organize the gamma oscillation. The simulation of Fig. 13 indicates that this is not necessarily so (although experimental evidence, Fig. 1, suggests a requirement for gap junctions). In Fig. 13, gap junction conductances were set to zero while the mean interval between random ectopic axonal current pulses

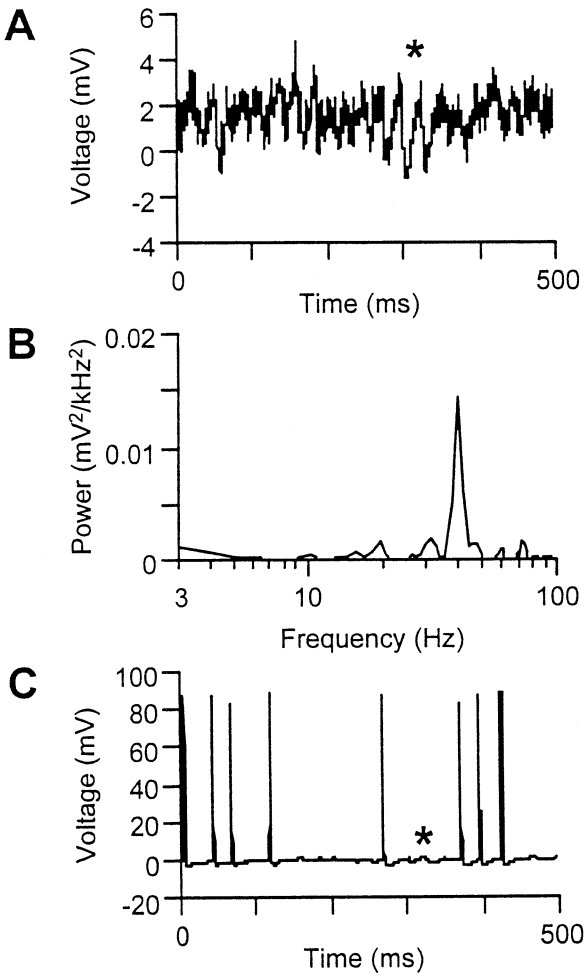

FIG. 11. Model: reducing gap junction conductance by 40% lead to short epochs of gamma oscillation, interspersed with periods lacking oscillation. Parameters otherwise as in Figs 2 and 3. (A) Local average potential of 224 pyramidal cells; ★ marks a brief epoch of 'clean' oscillation. (B) Power spectrum of the signal in A. There was a sharp peak at 40 Hz, but the amplitude was < 5% of that in Fig. 2. (C) Individual pyramidal cell; ★ marks a brief epoch of intracellular oscillation.

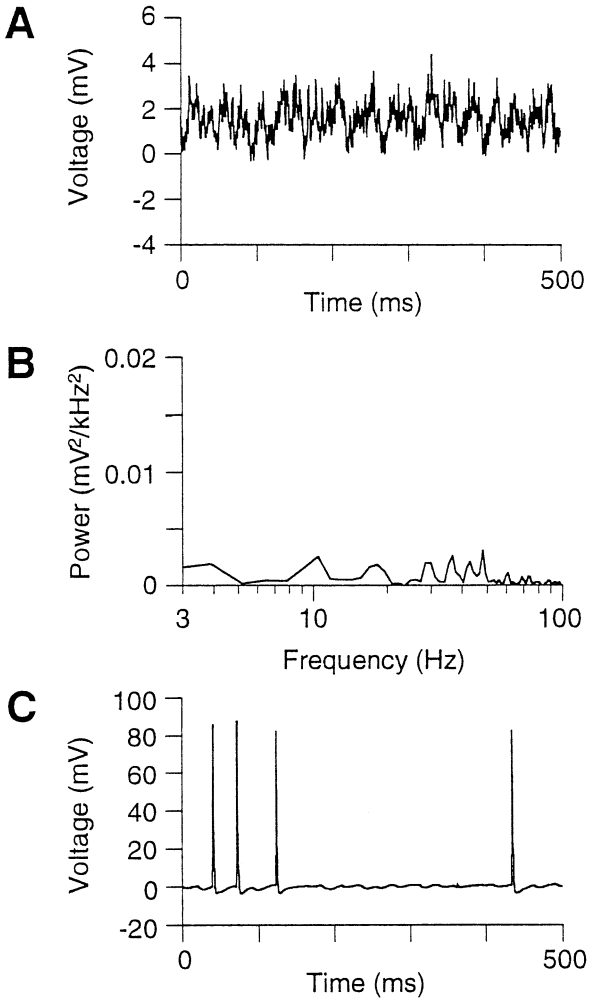

FIG. 12. Model: reducing gap junction conductance by 60% abolished the gamma oscillation. Parameters otherwise as in Figs 2 and 3. (A) Local average potential of 224 pyramidal cells. (B) Power spectrum of the signal in A. (C) Individual pyramidal cell.

was reduced from 65 to 20 ms. All other parameters were kept as in Fig. 2. Figure 13 shows that a synchronized population oscillation (48 Hz) still arose, with intermittent firing of the pyramidal cells (although at somewhat higher frequency than in Fig. 2). This result implies that the major effect of axon–axon gap junctions in our model is to amplify the axonal activity (by allowing axonal spikes to cross directly to other axons), rather than to organize the gamma-frequency rhythm. It is the IPSPs, in interneurons and in pyramidal cells, that organize the gamma rhythm. Interestingly, in the simulation of Fig. 13, synchrony of oscillations across the array is imperfect (mean phase lag 3.8 ms, not shown), unlike the simulation of Fig. 2 where gap junctions were used (phase lag < 1 ms).

Although the model can work without gap junctions, if the ectopic rate is high enough, the model cannot work when there are no ectopic spikes at all; there is then no activity in the axonal network to drive the interneurons. The interrelations between ectopic rates and gap junction conductances have been explored in more detail in a model of 4AP-induced ectopic activity (R. D. Traub, A. Bibbig, A. Piechotta, A. Draguhn and D. Schmitz, unpublished data); the effect of varying gap junctional density and ectopic rates was also explored, in a simpler model, in Traub *et al.*, 1999c.

Discussion

Summary of network mechanisms in the model of carbachol oscillations, and comparison with tetanically elicited oscillations

The following scheme illustrates the most important cellular events that were repeated cyclically to generate the simulated network oscillations in the present paper:

Synchronized fast IPSPs in pyramidal cells and interneurons
⇓
Decay of IPSPs
Random ectopic spikes in axons
⇓
Build-up of activity in network of pyramidal cell axons, dependent on random ectopic spikes and on gap junctions, which amplify the random activity
⇓
Synchronized AMPA-receptor mediated excitatory postsynaptic conductances in interneurons, with firing of many of them; some pyramidal cells also fire
⇓
Etc.

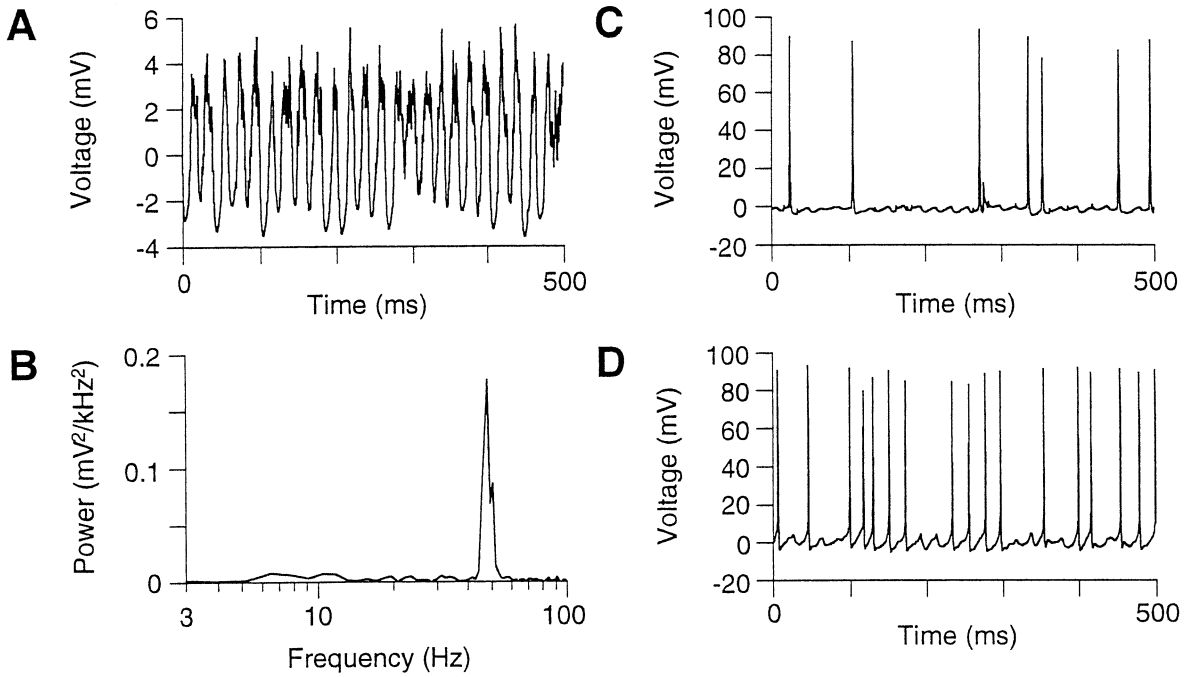

FIG. 13. Model: gamma oscillations could occur in the population, in the absence of axon–axon gap junctions, provided ectopic axonal spikes occurred at a sufficiently high frequency. Gap junction conductance was set to zero, and the mean interval between ectopic events in single pyramidal cell axons was decreased from 65 to 20 ms; parameters otherwise as in Figs 2 and 3. (A) Local average potential of 224 pyramidal cells. (B) Power spectrum of the signal in A. Note the large peak at 48 Hz. (C) Individual pyramidal cell. (D) Individual interneuron.

The scheme above shares some features with a model of tetanic stimulus-elicited gamma oscillations (Traub *et al*., 1997) in local networks, although there are differences as well. Probably the most important similarity concerns the structure of the interneuron network (mutual inhibition between interneurons, as well as inhibition of principal neurons), as well as the function of the interneuron network (tight locking of interneuron action potentials to population waves). More striking are the differences between the two sorts of gamma oscillations as follows.

(i) In the carbachol model, the driving conductances to pyramidal cells and to interneurons are not sufficient, in themselves, to ensure tonic firing at gamma frequency of the respective cell populations when chemical synapses are normally functioning. In the tetanic oscillation model, however, large tonic conductances were used in both cell types, as occurs experimentally (Whittington *et al*., 1997a). The tonic conductance in interneurons ensures the firing of inhibitory cells, even when AMPA receptor-mediated synaptic input to interneurons is blocked.

(ii) In the carbachol model, spontaneously generated ectopic action potentials, in the pyramidal cell axons, play a critical role in providing an AMPA-receptor mediated synaptic input to the interneurons that forces the latter to fire. This synaptic input substitutes for the tonic excitatory input to interneurons used in the tetanic oscillation model. The (theoretically) necessary frequency of ectopic action potentials is lower, when axon–axon gap junctions are present, as compared with the situation where such gap junctions are not present. The reason is that axon–axon gap junctions provide a form of amplification by allowing spikes to spread throughout the axonal plexus. Axon–axon gap junctions also could contribute to long-range synchrony of the gamma activity. Even with gap junctions, however, rather frequent ectopic spikes appear to be necessary. It is not known what biological factors might sustain ectopic axonal action potentials over a period of hours, the period over which carbachol-induced oscillations can occur experimentally.

In order for a population oscillation to occur, the interneurons need to be able to gate the activity of the pyramidal cell axons. This gating requires that either the axon–axon gap junctions, or the sites of ectopic spike generation (or both), are near to the axon initial segment. Additionally, if a build-up of axonal action potentials is to take place via gap junctions, this build-up will require a finite amount of time, ≈ 10 ms in our simulations. With an oscillation of 25 ms, IPSPs must then decay over ≈ 15 ms, forcing the model to use a small value for $\tau_{GABA(A)}$.

(c) In the tetanic oscillation model (Traub *et al*., 1997; Whittington *et al*., 1997a), pyramidal cell action potentials occur as IPSPs decay, with depolarizing influences derived from tonic excitatory conductances distributed over dendritic membrane. Action potentials are initiated in the axon initial segment (Traub *et al*., 1994), which is excited by dendritic currents. In the carbachol model, however, action potentials are initiated in the axon, distal to the initial segment: a specific prediction of this model. [Interestingly, the data of Colbert & Johnston (1996), on subicular pyramidal cells, suggest that, under all conditions, action potentials are initiated in the axon distal to the initial segment and are, in a sense, antidromic.] In the carbachol model, pyramidal cell IPSPs can be large enough so that the antidromic spikes successfully invade the soma only rarely, or not at all, accounting for the low frequency of pyramidal cell firing observed experimentally (Fisahn *et al*., 1998). This low frequency of pyramidal cell firing stands in contrast to the situation in tetanically induced oscillations (provided the tetanic stimulation is not applied too often), wherein pyramidal cells fire on most or all of the gamma waves, and where firing is presumed to be initiated orthodromically (Whittington *et al*., 1997a).

Implications for hippocampal gamma oscillations in vivo

The most novel aspect of the gamma-oscillation model described herein is the AMPA-receptor mediated excitation of interneurons by axonal network activity. We have recently shown how principal-cell

axonal network activity, synaptically driving interneurons, might also account for ≈200 Hz ripple oscillations *in vivo* (Traub & Bibbig, 2000). [The postulated role of inhibitory feedback in gating a gamma oscillation is, in contrast, present in many other models of population oscillations (e.g. Freeman, 1974).] To our knowledge, there are no data to indicate the presence of high rates of spontaneous ectopic action potentials under physiological conditions *in vivo*. Rather than providing an answer concerning ectopic spikes *in vivo*, our model poses a question: interneurons clearly participate in, and fire during, hippocampal gamma oscillations *in vivo* (Sik *et al*., 1995). Is the time course of excitation to these interneurons: (i) tonic, or varying at theta frequency (as suggested by Fig. 5 of Traub *et al*., 1996b); (ii) phasic at gamma frequency, by virtue of being gated by interneuronal network output, as in the present model; (iii) something else?

Acknowledgements

Supported by the Wellcome Trust, the Medical Research Council (UK) (Programme Grant G9901235), the Deutsche Forschungsgemeinschaft and the Human Frontier Science Program. We are grateful for helpful discussions with Dietmar Schmitz, Andreas Draguhn and Martin Vreugdenhil. A.B. thanks Günther Palm and Wayne Wickelgren for their continual support. R.D.T. is a Wellcome Principal Research Fellow.

Abbreviations

ACSF, artificial cerebrospinal fluid; AHP, afterhyperpolarization; AMPA, α-amino-3-hydroxy-5-methyl-4-isoxazole propionic acid; EEG, electroencephalogram; EPSP, excitatory postsynaptic potential; g_{Ca}, high-voltage-activated noninactivating Ca conductance; $g_{K(A)}$, transient inactivating K conductance; $g_{K(AHP)}$, slow Ca^{2+}-dependent afterhyperpolarization conductance; $g_{K(C)}$, voltage- and Ca^{2+}-dependent fast K conductance; $g_{K(DR)}$, delayed rectifier K conductance; GluR, glutamate receptor; $g_{Na(P)}$, persistent Na^+ conductance; g_{Na}, inactivating Na conductance; IPSC, inhibitory postsynaptic conductance; IPSP, inhibitory postsynaptic potential.

References

Avoli, M., Method, M. & Kawasaki, H. (1998) GABA-dependent generation of ectopic action potentials in the rat hippocampus. *Eur. J. Neurosci.*, **10**, 2714–2722.

Benson, D.M., Blitzer, R.D. & Landau, E.M. (1988) An analysis of the depolarization produced in guinea-pig hippocampus by cholinergic receptor stimulation. *J. Physiol. (Lond.)*, **404**, 479–496.

Buhl, E.H., Tamás, G. & Fisahn, A. (1998) Cholinergic activation and tonic excitation induce persistent gamma oscillations in mouse somatosensory cortex *in vitro*. *J. Physiol. (Lond.)*, **513**, 117–126.

Cantrell, A.R., Ma, J.Y., Scheuer, T. & Catterall, W.A. (1996) Muscarinic modulation of sodium current by activation of protein kinase C in rat hippocampal neurons. *Neuron*, **16**, 1019–1026.

Chapman, C.A. & Lacaille, J.-C. (1999) Cholinergic induction of theta-frequency oscillations in hippocampal inhibitory interneurons and pacing of pyramidal cell firing. *J. Neurosci.*, **19**, 8637–8645.

Charpak, S., Gähwiler, B., Do, K.Q. & Knöpfel, T. (1990) Potassium conductances in hippocampal neurons blocked by excitatory amino-acid transmitters. *Nature*, **347**, 765–767.

Colbert, C.M. & Johnston, D. (1996) Axonal action-potential initiation and Na^+ channel densities in the soma and axon initial segment of subicular pyramidal neurons. *J. Neurosci.*, **16**, 6676–6686.

Cole, A.E. & Nicoll, R.A. (1984) Characterization of a slow cholinergic post-synaptic potential recorded *in vitro* from rat hippocampal pyramidal cells. *J. Physiol. (Lond.)*, **352**, 173–188.

Csicsvari, J., Hirase, H., Czurko, A. & Buzsáki, G. (1998) Reliability and state-dependence of pyramidal cell-interneuron synapses in the hippocampus: an ensemble approach in the behaving rat. *Neuron*, **21**, 179–189.

Debanne, D., Guérineau, N.C., Gähwiler, B.H. & Thompson, S.M. (1997) Action-potential propagation gated by an axonal I_A-like K^+ conductance in hippocampus. *Nature*, **389**, 286–289.

Draguhn, A., Traub, R.D., Schmitz, D. & Jefferys, J.G.R. (1998) Electrical coupling underlies high-frequency oscillations in the hippocampus *in vitro*. *Nature*, **394**, 189–192.

Erdös, P. & Rényi, A. (1960) On the evolution of random graphs. *Publ. Math. Instit. Hungar. Acad. Sci.*, **5**, 17–61.

Faulkner, H.J., Traub, R.D. & Whittington, M.A. (1998) Disruption of synchronous gamma oscillations in the rat hippocampal slice: a common mechanism of anaesthetic drug action. *Br. J. Pharmacol.*, **125**, 483–492.

Fellous, J.-M. & Sejnowski, T.J. (2000) Cholinergic induction of oscillations in the hippocampal slice in the slow (0.5–2 Hz), theta (5–12 Hz), and gamma (35–70 Hz) bands. *Hippocampus*, **10**, 187–197.

Fisahn, A. (1999) An investigation into cortical gamma frequency oscillations *in vitro.* PhD Dissertation, Oxford University, Oxford.

Fisahn, A., Pike, F.G., Buhl, E.H. & Paulsen, O. (1998) Cholinergic induction of network oscillations at 40 Hz in the hippocampus *in vitro*. *Nature*, **394**, 186–189.

Frazier, C.J., Rollins, Y.D., Breese, C.R., Leonard, S., Freedman, R. & Dunwiddie, T.V. (1998) Acetylcholine activates an alpha-bungarotoxin-sensitive nicotinic current in rat hippocampal interneurons, but not pyramidal cells. *J. Neurosci.*, **18**, 1187–1195.

Freeman, W.J. (1974) Average transmission distance from mitral-tufted to granule cells in olfactory bulb. *Electroenceph. Clin. Neurophysiol.*, **36**, 609–618.

French, C.R., Sah, P., Buckett, K.J. & Gage, P.W. (1990) A voltage-dependent persistent sodium current in mammalian hippocampal neurons. *J. Gen. Physiol.*, **95**, 1139–1157.

Fukuda, T. & Kosaka, T. (2000) Gap junctions linking the dendritic network of GABAergic interneurons in the hippocampus. *J. Neurosci.*, **20**, 1519–1528.

Gähwiler, B.H. & Brown, D.A. (1987) Muscarine affects calcium-currents in rat hippocampal pyramidal cells in vitro. *Neurosci. Lett.*, **76**, 301–306.

Galarreta, M. & Hestrin, S. (1999) A network of fast-spiking cells in the neocortex connected by electrical synapses. *Nature*, **402**, 72–75.

Gho, M., King, A.E., Ben-Ari, Y. & Cherubini, E. (1986) Kainate reduces two voltage-dependent potassium conductances in rat hippocampal neurons in vitro. *Brain Res.*, **385**, 411–414.

Gibson, J.R., Beierlein, M. & Connors, B.W. (1999) Two networks of electrically coupled inhibitory neurons in neocortex. *Nature*, **402**, 75–79.

Gray, C.M. & Singer, W. (1989) Stimulus-specific neuronal oscillations in orientation columns of cat visual cortex. *Proc. Natl Acad. Sci. USA,* **86**, 1698–1702.

Kawaguchi, Y. (1997) Selective cholinergic modulation of cortical GABAergic cell subtypes. *J. Neurophysiol.*, **78**, 1743–1747.

Knöpfel, T., Vranesic, I., Gähwiler, B. & Brown, D.A. (1990) Muscarinic and β-adrenergic depression of the slow Ca^{2+} -activated potassium conductance in hippocampal CA3 pyramidal cells is not mediated by a reduction of depolarization-induced cytosolic Ca^{2+} transients. *Proc. Natl Acad. Sci. USA*, **87**, 4083–4087.

Kramis, R., Vanderwolf, C.H. & Bland, B.H. (1975) Two types of hippocampal rhythmical slow activity (RSA) in both the rabbit and the rat: relations to behavior and effects of atropine, diethyl ether, urethane and pentobarbital. *Exp. Neurol.*, **49**, 58–85.

Levey, A.I., Edmunds, S.M., Hersch, S.M., Wiley, R.G. & Heilman, C.J. (1995) Light and electron microscopic study of m2 muscarinic acetylcholine receptor in the basal forebrain of the rat. *J. Comp. Neurol.*, **351**, 339–356.

Li, X.-G., Somogyi, P., Ylinen, A. & Buzsáki, G. (1994) The hippocampal CA3 network: an in vivo intracellular labeling study. *J. Comp. Neurol.*, **339**, 181–208.

Maccaferri, G. & McBain, C.J. (1996) The hyperpolarization-activated current (I_h) and its contribution to pacemaker activity in rat CA1 hippocampal stratum oriens-alveus interneurones. *J. Physiol. (Lond.)*, **497**, 119–130.

MacDonald, K.D., Brett, B. & Barth, D.S. (1996) Inter- and intra-hemispheric spatiotemporal organization of spontaneous electrocortical oscillations. *J. Neurophysiol.*, **76**, 423–437.

Madison, D.V., Lancaster, B. & Nicoll, R.A. (1987) Voltage clamp analysis of cholinergic action in the hippocampus. *J. Neurosci.*, **7**, 733–741.

Mittman, T., Linton, S.M., Schwindt, P. & Crill, W. (1997) Evidence for persistent Na^+ current in apical dendrites of rat neocortical neurons from imaging of Na^+-sensitive dye. *J. Neurophysiol.*, **78**, 1188–1192.

Nakajima, Y., Nakajima, S., Leonard, R.J. & Yamaguchi, K. (1986) Acetylcholine raises excitability by inhibiting the fast transient potassium current in cultured hippocampal neurons. *Proc. Natl Acad. Sci. USA*, **83**, 3022–3026.

Pawelzik, H., Hughes, D. & Thomson, A.M. (1998) Single-axon IPSPs as generated by identified horizontal oriens/alveus interneurones in

simultaneously recorded postsynaptic pyramidal cells of adult rat hippocampus in vitro. *Soc. Neurosci. Abstr.*, **24**, 1811.

Perez Velazquez, J.L., Han, D. & Carlen, P.L. (1997) Neurotransmitter modulation of gap junctional communication in the rat hippocampus. *Eur. J. Neurosci.*, **9**, 2522–2531.

Rodriguez-Moreno, A. & Lerma, J. (1998) Kainate receptor modulation of GABA release involves a metabotropic function. *Neuron*, **20**, 1211–1218.

Roelfsema, P.R., König, P., Engel, A.K., Sireteanu, R. & Singer, W. (1994) Reduced synchronization in the visual cortex of cats with strabismic amblyopia. *Eur. J. Neurosci.*, **6**, 1645–1655.

Scanziani, M., Gähwiler, B.H. & Thompson, S.M. (1995) Presynaptic inhibition of excitatory synaptic transmission by muscarinic and metabotropic glutamate receptor activation in the hippocampus: are Ca^{2+} channels involved? *Neuropharmacology*, **34**, 1549–1557.

Segal, M. (1989) Presynaptic cholinergic inhibition in hippocampal cultures. *Synapse*, **4**, 305–312.

Sik, A., Penttonen, M., Ylinen, A. & Buzsáki, G. (1995) Hippocampal CA1 interneurons: an *in vivo* intracellular labeling study. *J. Neurosci.*, **15**, 6651–6665.

Soltesz, I. & Deschênes, M. (1993) Low- and high-frequency membrane potential oscillations during theta activity in CA1 and CA3 pyramidal neurons of the rat hippocampus under ketamine-xylazine anesthesia. *J. Neurophysiol.*, **70**, 97–116.

Stasheff, S.F., Mott, D.D. & Wilson, W.A. (1993) Axon terminal hyperexcitability associated with epileptogenesis in vitro. II. Pharmacological regulation by NMDA and $GABA_A$ receptors. *J. Neurophysiol.*, **70**, 976–984.

Storm, J. (1988) Temporal integration by a slowly inactivating K^+ current in hippocampal neurons. *Nature*, **336**, 379–381.

Tamás, G., Buhl, E.H., Lörincz, A. & Somogyi, P. (2000) Proximally targeted GABAergic synapses and gap junctions precisely synchronize cortical interneurons. *Nature Neurosci.*, **3**, 366–371.

Towers, S.K., LeBeau, F. & Buhl, E.H. (2000) Synaptic and non-synaptic mechanisms of oscillatory network activity in the rat dentate gyrus in vitro. *J. Physiol. (Lond)*, **523**, 186P.

Traub, R.D. & Bibbig, A. (2000) A model of high-frequency ripples in the hippocampus, based on synaptic coupling plus axon-axon gap junctions between pyramidal neurons. *J. Neurosci.*, **20**, 2086–2093.

Traub, R.D. & Miles, R. (1995) Pyramidal cell-to-inhibitory cell spike transduction explicable by active dendritic conductances in inhibitory cell. *J. Comput. Neurosci.*, **2**, 291–298.

Traub, R.D., Jefferys, J.G.R., Miles, R., Whittington, M.A. & Tóth, K. (1994) A branching dendritic model of a rodent CA3 pyramidal neurone. *J. Physiol. (Lond.)*, **481**, 79–95.

Traub, R.D., Colling, S.B. & Jefferys, J.G.R. (1995) Cellular mechanisms of 4-aminopyridine-induced synchronized after-discharges in the rat hippocampal slice. *J. Physiol. (Lond.)*, **489**, 127–140.

Traub, R.D., Borck, C., Colling, S.B. & Jefferys, J.G.R. (1996a) On the structure of ictal events *in vitro*. *Epilepsia*, **37**, 879–891.

Traub, R.D., Whittington, M.A., Colling, S.B., Buzsáki, G. & Jefferys, J.G.R. (1996b) Analysis of gamma rhythms in the rat hippocampus *in vitro* and *in vivo*. *J. Physiol. (Lond.)*, **492**, 471–484.

Traub, R.D., Jefferys, J.G.R. & Whittington, M. (1997) Simulation of gamma rhythms in networks of interneurons and pyramidal cells. *J. Comput. Neurosci.*, **4**, 141–150.

Traub, R.D., Jefferys, J.G.R. & Whittington, M. (1999a). *Fast Oscillations in Cortical Circuits*. MIT Press, Cambridge, MA.

Traub, R.D., Whittington, M.A., Buhl, E.H., Jefferys, J.G.R. & Faulkner, H.J. (1999b) On the mechanism of the $\gamma \rightarrow \beta$ frequency shift in neuronal oscillations induced in rat hippocampal slices by tetanic stimulation. *J. Neurosci.*, **19**, 1088–1105.

Traub, R.D., Schmitz, D., Jefferys, J.G.R. & Draguhn, A. (1999c) High-frequency population oscillations are predicted to occur in hippocampal pyramidal neuronal networks interconnected by axo-axonal gap junctions. *Neuroscience*, **92**, 407–426.

Traub, R.D., Bibbig, A., Fisahn, A. & Buhl, E.H. (1999d) Model of carbachol- and kainate-induced 40 Hz oscillations in vitro, dependent on AMPA and $GABA_A$ receptors, as well as on axon-axon gap junctions. *Soc. Neurosci. Abstr.*, **25**, 903.

Wang, X.-J. & Buzsáki, G. (1996) Gamma oscillation by synaptic inhibition in a hippocampal interneuronal network model. *J. Neurosci.*, **16**, 6402–6413.

White, J.A., Chow, C.C., Ritt, J., Soto-Treviño, C. & Kopell, N. (1998) Synchronization and oscillatory dynamics in heterogeneous, mutually inhibited neurons. *J. Comput. Neurosci.*, **5**, 5–16.

Whittington, M.A., Jefferys, J.G.R. & Traub, R.D. (1996) Effects of intravenous anaesthetic agents on fast inhibitory oscillations in the rat hippocampus *in vitro*. *Br. J. Pharmacol.*, **118**, 1977–1986.

Whittington, M.A., Stanford, I.M., Colling, S.B., Jefferys, J.G.R. & Traub, R.D. (1997a) Spatiotemporal patterns of γ frequency oscillations tetanically induced in the rat hippocampal slice. *J. Physiol. (Lond.)*, **502**, 591–607.

Whittington, M.A., Traub, R.D. & Jefferys, J.G.R. (1995) Synchronized oscillations in interneuron networks driven by metabotropic glutamate receptor activation. *Nature*, **373**, 612–615.

Whittington, M.A., Traub, R.D., Faulkner, H.J., Stanford, I.M. & Jefferys, J.G.R. (1997b) Recurrent excitatory postsynaptic potentials induced by synchronized fast cortical oscillations. *Proc. Natl Acad. Sci. USA*, **94**, 12198–12203.

Ylinen, A., Bragin, A., Nádasdy, Z., Jandó, G., Szabó, I., Sik, A. & Buzsáki, G. (1995) Sharp wave-associated high-frequency oscillation (200 Hz) in the intact hippocampus: network and intracellular mechanisms. *J. Neurosci.*, **15**, 30–46.